

Oxidation and Ablation Resistance of SiC/ZrB₂-SiC-B₄C Coatings for C/SiC Composites

Zhang Baopeng, Yu Xinmin, Liu Junpeng, Liu Wei, Huo Pengfei

Aerospace Institute of Advanced Materials & Processing Technology, Beijing 100074, China

Abstract: Double-layered SiC/ZrB₂-SiC-B₄C coatings were fabricated by chemical vapor deposition (CVD) and slurry painting-sintering methods. The naked, single-SiC coated and SiC/ZrB₂-SiC-B₄C double-layered C/SiC composites were oxidized at 1500 °C and ablated under a heat flux of 4.2 MW/m². The results indicate that the slurry-painted ZrB₂-SiC-B₄C coating is dense and intact, which has a surface roughness R_a of ~1 μm and the porosity of ~4.2%. After oxidation at 1500 °C for 30 h, the mass loss ratio of SiC/ZrB₂-SiC-B₄C coated C/SiC composite is ~10%. The oxidation scale on the coating surface is compact without obvious cracking. After ablating for 20 s, the linear and mass ablation rates of SiC/ZrB₂-SiC-B₄C coating are 1.0±0.3 μm/s and 1.1±0.2 mg/s, decreased by 75.0% and 50.0% relative to those of the SiC coating, respectively. The formed ZrO₂-SiO₂ scale provides a protection against the mechanical erosion from the flame.

Key words: C/SiC composites; coating; slurry painting; oxidation; ablation

Carbon/silicon-carbide (C/SiC) composites are attractive thermal structure materials widely used in the aeronautical and aerospace fields because of their excellent properties such as low density, high specific strength and elastic modulus, high thermal conductivity, good abrasive resistance and high thermal stability^[1-4]. However, oxidation and ablation are always considered as key problems that limit the aerospace applications of C/SiC composites^[5,6]. Applying coatings on C/SiC composite surface is an effective method to improve oxidation and ablation resistance^[7-9].

The ultra-high temperature ceramics (UHTCs), such as borides (ZrB₂, HfB₂) and carbides (ZrC), are ideal coating materials for C/SiC composites at ultra-high temperatures due to their extremely high melting points (above 3000 °C) and the corresponding oxides with sufficiently high melting points (2680 °C for ZrO₂ and 2758 °C for HfO₂)^[10-14]. However, the poor oxidation resistance of UHTCs limits their operating temperature. To solve this problem, the addition of silicon-based phases (SiC, MoSi₂) is often used for oxidation protection, since the formed SiO₂ can effectively seal the pores and cracks occurred in the coating below 1800 °C^[15-17]. It is reported that ZrB₂-SiC based ceramic coatings have

excellent oxidation and ablation resistance. After oxidation at 1500 °C for 10 h, the mass loss ratio of SiC/ZrB₂-SiC double-layered C/SiC composite is around 5.3%^[18]. Under the condition of oxygen-acetylene ablation at ~1727 °C for 40 s, the linear and mass ablation rates of ZrB₂-SiC coated C/SiC composites are 4.4×10⁻³ mm/s and 6.2×10⁻⁵ g/s, respectively^[19].

Currently, three methods including chemical vapor deposition (CVD), atmospheric plasma spraying (APS) and slurry painting are mainly used to prepare ultra-high temperature ceramic coatings on C/SiC composites^[18,20]. CVD-prepared coatings have the advantages of low porosity and high bonding strength. However, the low deposition rate (~1 μm/h) and high cost are the disadvantages of CVD process. APS-prepared coatings are formed by the stacking of flattened particles, which results in lamellar structure. The deposition efficiency of APS process is usually higher (~100 μm/min), while there are more pores (porosity>10%) and defects in the APS coatings. Besides, it is difficult for both CVD and APS methods to deposit uniform coatings on the surface of large components with complicated geometries, such as combustion chambers and nozzles. In comparison, slurry painting

Received date: December 03, 2019

Corresponding author: Zhang Baopeng, Ph. D., Aerospace Institute of Advanced Materials & Processing Technology, Beijing 100074, P. R. China, Tel: 0086-10-68743595, E-mail: bhzbp1129@buaa.edu.cn

Copyright © 2020, Northwest Institute for Nonferrous Metal Research. Published by Science Press. All rights reserved.

technique is particularly attractive for its low cost, simple process, low equipment requirement, and easy control of coating thickness. More importantly, the coatings can be uniformly prepared on the large-sized components in one slurry painting process.

For these reasons, the development of slurry-painted coatings with superior resistance to oxidation and ablation is imperative for the development of next-generation combustion chambers. However, little literature is available for the oxidation and ablation characterization of slurry-painted coatings. Besides, the relevant oxidation and ablation behavior of the coatings are rather restricted and required to be explored, especially in the slurry painting case. In this study, the ZrB_2 -SiC- B_4C ceramic top coat was prepared by slurry painting method. To narrow the thermal expansion coefficient between ZrB_2 and C/SiC composites, the SiC and B_4C were added in the coating. Meanwhile, a SiC bond coat was deposited by CVD technique. In order to analyze how the composition of coatings affects the anti-oxidation and anti-ablation properties, we compared the oxidation and ablation of naked, single-SiC coated and SiC/ ZrB_2 -SiC- B_4C coated C/SiC composites. The corresponding oxidation dynamics and ablation rates were quantitatively characterized, with the analysis provided to describe its oxidation and ablation processes. The double-layered SiC/ ZrB_2 -SiC- B_4C showed excellent anti-oxidation and anti-ablation abilities.

1 Experiment

1.1 Coating preparation

2D C/SiC composite with a density of $1.80 \text{ g}\cdot\text{cm}^{-3}$ was used as the substrate for coating preparation. The composites were shaped into the size of $30 \text{ mm}\times 25 \text{ mm}\times 10 \text{ mm}$ for oxidation tests and $\Phi 30 \text{ mm}\times 10 \text{ mm}$ for ablation tests. The samples were then cleaned with ethanol and dried at $100 \text{ }^\circ\text{C}$ for 2 h.

The SiC coatings were deposited at $1050 \text{ }^\circ\text{C}$ by CVD in vacuum using methyltrichlorosilane (MTS, CH_3SiCl_3)/hydrogen (H_2) as reactant species. The raw materials of slurry for preparing ZrB_2 -SiC- B_4C top coat were as follows: 30wt%~40wt% B ($25 \text{ }\mu\text{m}$), 20wt%~30wt% Si ($25 \text{ }\mu\text{m}$), 10wt%~20wt% ZrB_2 ($38 \text{ }\mu\text{m}$) and 40wt%~50wt% phenolic resin, which were all of analytical grade and thoroughly mixed by tumbling. The slurry was then brushed on the surface of samples through a paintbrush. After being dried at $130 \text{ }^\circ\text{C}$ for 2 h, the brushed samples were heated at $1500 \text{ }^\circ\text{C}$ for 2 h in a carbon tube furnace with argon atmosphere. Subsequently, the slurry painting-sintering process was repeated for one more time, and the ZrB_2 -SiC- B_4C coating was formed. For comparison, the C/SiC and single-SiC coated C/SiC were adopted for oxidation and ablation experiments.

1.2 Oxidation test

The oxidation experiments of uncoated, SiC coated and SiC/ ZrB_2 -SiC- B_4C double-layered C/SiC composites were carried out in a high temperature tubular furnace in static air at

$1500 \text{ }^\circ\text{C}$. Samples were taken out from the furnace at intervals, air-cooled to room temperature, and then weighed using an electronic balance with a sensitivity of $\pm 0.1 \text{ mg}$. The following formula is used to calculate the mass change ratio of the samples:

$$\Delta m = (m_1 - m_0) / m_0 \times 100\% \quad (1)$$

where Δm is the mass change ratio, m_0 and m_1 are the mass of the samples before and after oxidation, respectively.

1.3 Ablation test

The ablation tests were performed using an oxyacetylene torch according to GJB 323A-96 with a heat flux of $4.2 \text{ MW}/\text{m}^2$. The flux and pressure of O_2 were $0.62 \text{ m}^3/\text{h}$ and 0.4 MPa , and those of C_2H_2 were $0.76 \text{ m}^3/\text{h}$ and 0.095 MPa , respectively. The as-prepared specimens were exposed to the oxyacetylene flame for 20 s with the ablation distance of 10 mm. The linear and mass ablation rates of the specimens were calculated in terms of the following equations:

$$R_l = (l_0 - l_1) / t \quad (2)$$

$$R_m = (m_0 - m_1) / t \quad (3)$$

where R_l and R_m are linear and mass ablation rate, respectively; l_0 and m_0 are the height and mass of the sample before ablation, respectively; l_1 is the sample height in the central zone of the ablation; m_1 is the sample mass after ablation; t is the ablation time.

1.4 Coating characterization

The surface and cross-section morphologies of the specimens were characterized by a field-emission scanning electron microscopy (Supra 55, ZEISS) equipped with the back-scattered electron (BSE) detector and energy dispersive X-ray spectrum (EDS). The porosity of coatings was measured using the image analysis method. The phase constituents of the coated specimens were identified by X-ray diffraction (XRD, Rigaku D/max 2500PC) using $\text{Cu K}\alpha$ radiation. With the step size of $6^\circ/\text{min}$, the 2θ was scanned from 10° to 90° .

2 Results

2.1 As-prepared coatings

Fig.1a shows the SEM image of the surface morphology of as-prepared ZrB_2 -SiC- B_4C coating. It is noted that the slurry-painted coating surface is dense and intact. The pores and cracks are hardly found on the coating surface. Fig.1b is the back-scattered electron (BSE) image of the cross-section of SiC/ ZrB_2 -SiC- B_4C double-layered coating. The white layer deposited on C/SiC composite is the SiC bond coat with the thickness of $\sim 40 \text{ }\mu\text{m}$. The top coat of ZrB_2 -SiC- B_4C coating has a thickness of $\sim 60 \text{ }\mu\text{m}$, which is fabricated by two cycles of slurry painting and sintering processes while the thickness increases around $30 \text{ }\mu\text{m}$ after each cycle. The surface roughness R_a of ZrB_2 -SiC- B_4C coating is $\sim 1 \text{ }\mu\text{m}$, and the porosity is measured as $\sim 4.2\%$. Besides, there are no delamination cracks noticeable throughout the ZrB_2 -SiC- B_4C layer. The slurry-painted coating surface is detected by XRD to identify the phase constituents. Referring to the JCPDS

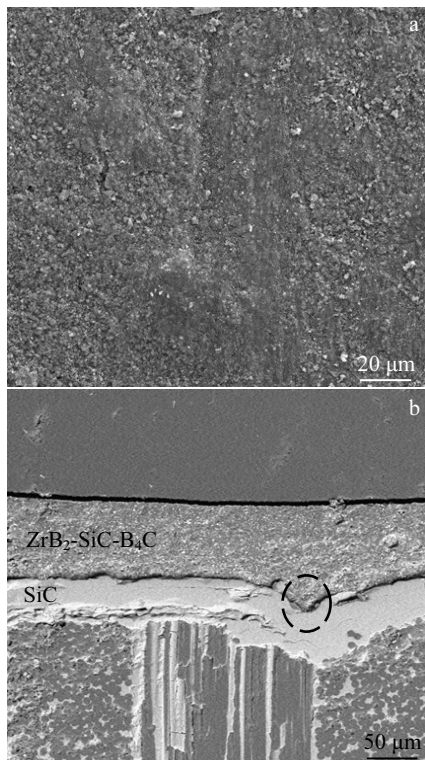


Fig.1 Surface (a) and cross-section (b) morphologies of the as-prepared SiC/ZrB₂-SiC-B₄C coatings

cards, the coating is composed of ZrB₂, SiC, and B₄C phases, as shown in Fig.2a.

Fig.3 shows the SEM images of surface morphology of the SiC coating fabricated by CVD method. From the low magnification image of Fig.3a, some cracks are observed on the coating surface, which may be attributed to the occurrence of thermal stress during cooling. As magnified in Fig.3b, the surface microstructure of SiC coating is characterized by micro-sized protuberances formed by the pure SiC deposition^[21]. Compared with SiC/ZrB₂-SiC-B₄C coating, the thickness of this single SiC coating deposited on C/SiC composite is ~100 μm. Fig.2b displays the XRD pattern of SiC coating deposited by CVD. According to the JCPDS card, the SiC coating is mainly composed of cubic β-SiC.

2.2 Oxidation property of the as-prepared specimens

Fig.4 presents the mass change Δm plotted as a function of the oxidation time t , which yields foremost insights into the oxidation dynamics of the specimens at 1500 °C. For the single SiC and double-layered SiC/ZrB₂-SiC-B₄C coatings, the oxidation curves tend to be parabolic. As for the naked C/SiC composite, the mass loss ratio increases rapidly and reaches to ~45.8% after oxidation for only 7 h. After oxidation for 10 h, the mass loss ratio reaches to a maximum of ~46.0%. Subsequently, the oxidation curve presents a rising tendency. After oxidation at 1500 °C for 30 h, the mass loss ratio of

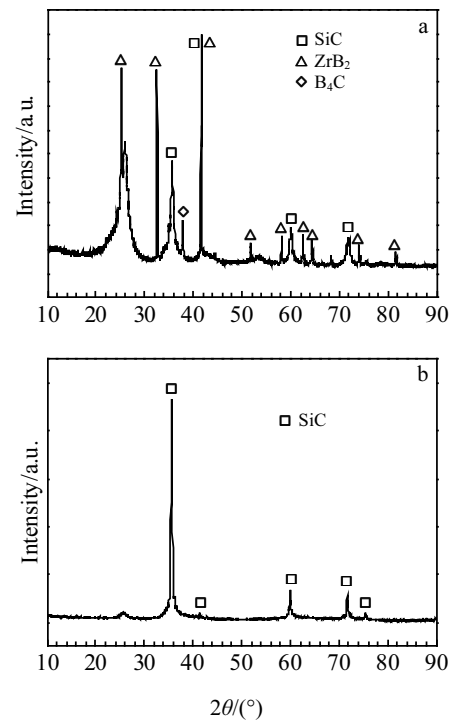


Fig.2 XRD patterns of the as-prepared ZrB₂-SiC-B₄C (a) and SiC (b) coatings

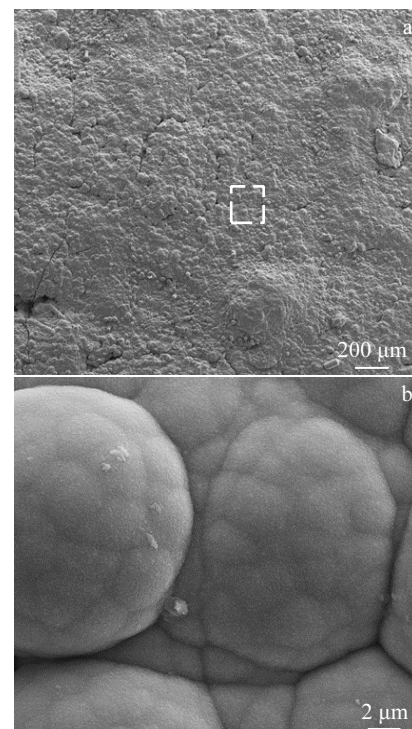


Fig.3 Surface morphologies of the SiC coating fabricated by CVD method with low (a) and high (b) magnification

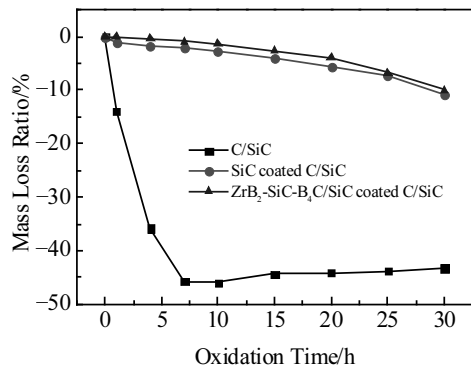


Fig.4 Isothermal oxidation curves of C/SiC composites with different coatings in air at 1500 °C

SiC/ZrB₂-SiC-B₄C coated C/SiC composite is measured as ~10.0%, which is slightly lower than that of the SiC coated C/SiC (~10.7%) and much lower than that of the C/SiC composite (~43.3%).

Fig.5 shows the surface and cross-section morphologies of naked, SiC coated and SiC/ZrB₂-SiC-B₄C coated C/SiC composites after oxidation at 1500 °C for 30 h. For uncoated C/SiC composite, the carbon fibers are severely oxidized into large holes, as shown in Fig.5a. High magnification morphology reveals that the smooth glass forms in the specimen. According to the EDS result, this glass phase consists of 37.25at% Si and 62.75at% O, as shown in Table 1, indicating that the SiC ceramic matrix has been oxidized. As for the SiC coated C/SiC composite, a glass layer forms with some defects such as microcracks and pinholes shown in Fig.5c.

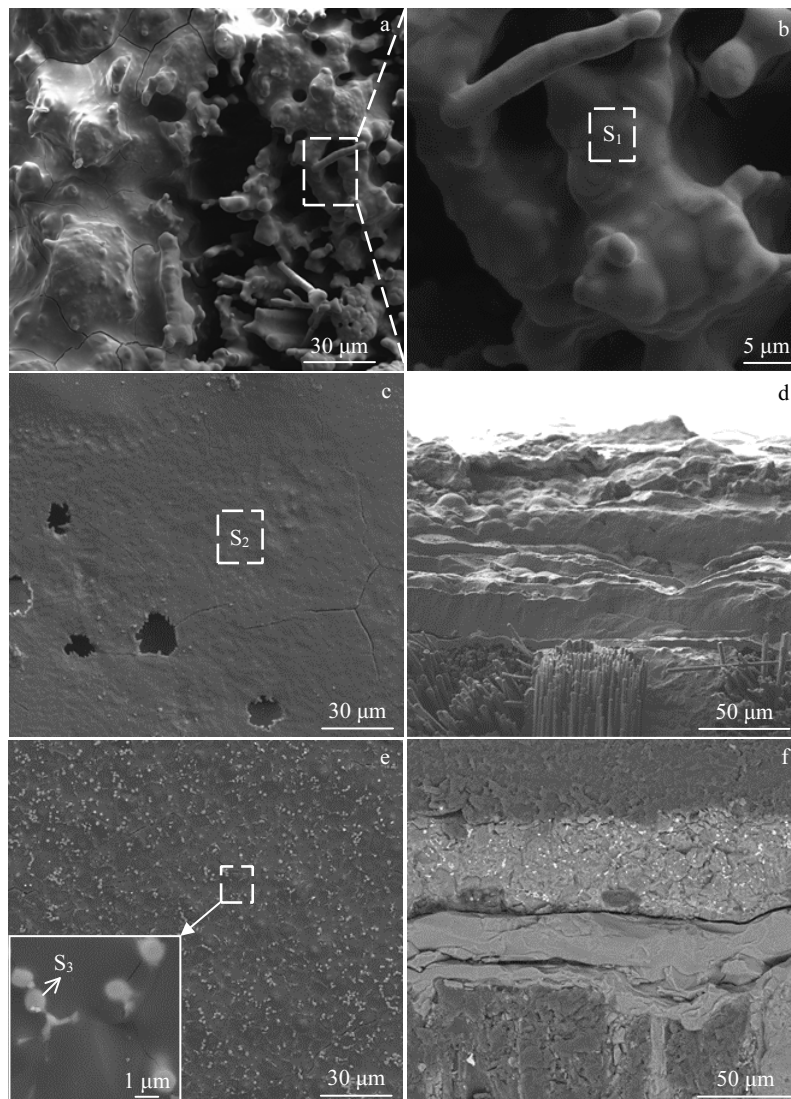


Fig.5 Surface and cross-section morphologies of the specimens after oxidation at 1500 °C for 30 h: (a, b) C/SiC, (c, d) SiC coated C/SiC, and (e, f) SiC/ZrB₂-SiC-B₄C coated C/SiC

EDS analysis of region S_2 shows that the vitreous oxidation products are composed of 38.56at% Si and 61.44at% O. After the oxidation test, the thickness of this oxide scale is about 80 μm . The BSE image of $\text{ZrB}_2\text{-SiC-B}_4\text{C}$ coating surface after oxidation is illustrated in Fig.5e. It is noted that the coating surface is glassy and dense. Apart from the amorphous phase, a mass of grey particles also exist in the coating, as depicted in Fig.5e. On the basis of EDS analysis, the circled phase is comprised of Zr, Si and O, of which the elemental compositions are quantitatively provided in Table 1. Meanwhile, the surrounding glass appears chemically homogeneous. After isothermal oxidation at 1500 $^\circ\text{C}$ for 30 h, the thickness of the oxide scale decreases to around 65 μm .

2.3 Ablation property of the as-prepared specimens

To evaluate the ablation resistance of C/SiC composites with different coatings, the specimens were tested at a heat flux of 4.2 MW/m^2 with the ablation distance of 10 mm. The corresponding maximum temperature was measured to be ~ 2200 $^\circ\text{C}$. Fig.6 displays the OM images of the samples

before and after ablation for 20 s. Some pores and the traces of carbon fibers are observed on the non-ablated C/SiC surface, while the surfaces of SiC and $\text{ZrB}_2\text{-SiC-B}_4\text{C}$ coatings are uniform and intact. The linear and mass ablation rates of these specimens after ablation for 20 s are shown in Fig.7. The linear and mass ablation rates are positive, indicating the thickness reduction and mass loss after ablation.

Table 1 EDS analysis of the composition of the marked regions $S_1\sim S_3$ in Fig.5 and regions S_4 and S_5 in Fig.8 (at%)

Region	C	O	Si	Zr
S_1	-	62.75	37.25	-
S_2	-	61.44	38.56	-
S_3	-	65.96	5.07	28.97
S_4	30.65	12.23	57.11	-
S_5	-	68.01	3.84	28.15

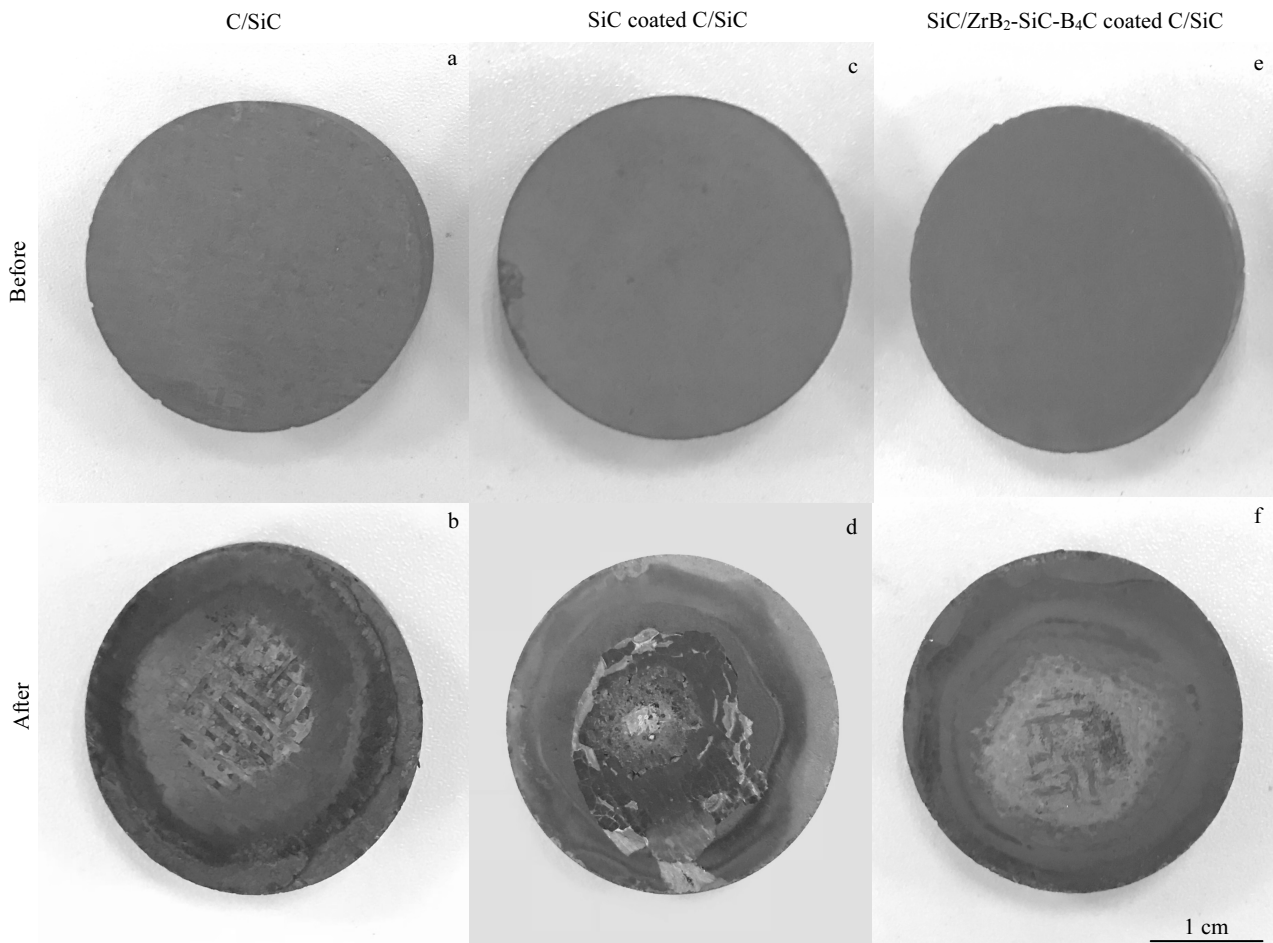


Fig.6 OM images of the specimens before (a, c, e) and after (b, d, f) ablation for 20 s under the heat flux of 4.2 MW/m^2 : (a, b) C/SiC, (c, d) SiC coated C/SiC, and (e, f) SiC/ZrB₂-SiC-B₄C coated C/SiC

It is observed in Fig.6b that the ablation center of naked C/SiC composite is severely damaged. The corresponding linear and mass ablation rates are $6.0\pm 0.4 \mu\text{m/s}$ and $5.7\pm 0.3 \text{ mg/s}$, respectively. The single-SiC coated C/SiC is damaged due to the ablation, leading to obvious ablation craters on the surface (Fig.6d), which indicates that the single SiC coating can not provide prolonged ablation protection for C/SiC composites. Compared with naked C/SiC composite, the linear and mass ablation rates of SiC coated C/SiC are reduced by 33.3% and 61.4%, respectively. The macrograph of the SiC/ZrB₂-SiC-B₄C coated C/SiC composite after ablation is shown in Fig.6f. The central area of the ablation on the coating surface turns to grey. As expected, the double-layered coating is basically integrated after ablation. In contrast to the SiC coated C/SiC composite, the linear and mass ablation rates of SiC/ZrB₂-SiC-B₄C coated C/SiC decrease by 75.0% and 50.0%, respectively, revealing a significant improvement in ablation resistance.

Fig.8 shows the central surface images of the specimens after ablation. It can be seen from Fig.8a that the carbon fibers in the naked C/SiC composite are obviously oxidized during ablation. The single SiC coating has been destructed, resulting in the exposure of C/SiC composites, which is evidenced by the bared and oxidized carbon fibers shown in Fig.8b. The residual glassy coating is mainly composed of 30.65at% C, 12.23at% O and 57.11at% Si (region S₄ in Fig.8b). The existence of C element suggests that the thickness of this residual coating is extremely thin. In addition, the ablation craters (denoted by white arrows in Fig.8b) are clearly observed on the surface of the glassy coating. Fig.8c shows the SEM image of the central surface area of SiC/ZrB₂-SiC-B₄C coating subjected to the highest heat flux during ablation. It is noticed that the surface becomes rough and porous after ablation. Fig.8d reveals that the particles are surrounded and connected by the glassy phase, forming a network microstructure. According to the

EDS result in Table 1, the coating is mainly comprised of 68.01at% O, 3.84at% Si and 28.15at% Zr (region S₅ in Fig.8d), confirming the formation of protective oxides of ZrO₂-SiO₂ on the surface.

3 Discussion

3.1 Microstructure of the coating

During the high-temperature sintering process at 1500 °C, the boron and liquid silicon react with the carbon derived from the pyrolysis of phenolic resin to form B₄C and SiC constituents. Meanwhile, the ZrB₂ phase retains in the coating, as proved by the XRD pattern in Fig.2a. It is observed that the ZrB₂ phase is distributed in the ceramic coating. Generally, the microstructure of slurry-painted coating is relatively loose with many pores. However, the ZrB₂-SiC-B₄C was made by double paintings followed by sintering each time. For this double-layered ZrB₂-SiC-B₄C coating, as shown in Fig.1, the coating surface is dense and compact without pinholes. Many factors, including the volume shrinkage of phenolic resin, and the thermal mismatch between the coating and the substrate, may result in defects in the coatings. Since the coating is prepared by two cycles of slurry painting and sintering, the latter layer can eliminate parts of the defects in the former layer. Furthermore, there is no thermal expansion mismatch between the former and the latter layers. Thus, the ZrB₂-SiC-B₄C coating shows a high integrity, which can be beneficial for the oxidation and ablation resistance.

3.2 Oxidation mechanisms of the specimens

When the samples are oxidized in air at 1500 °C for 30 h, the following reactions occur:

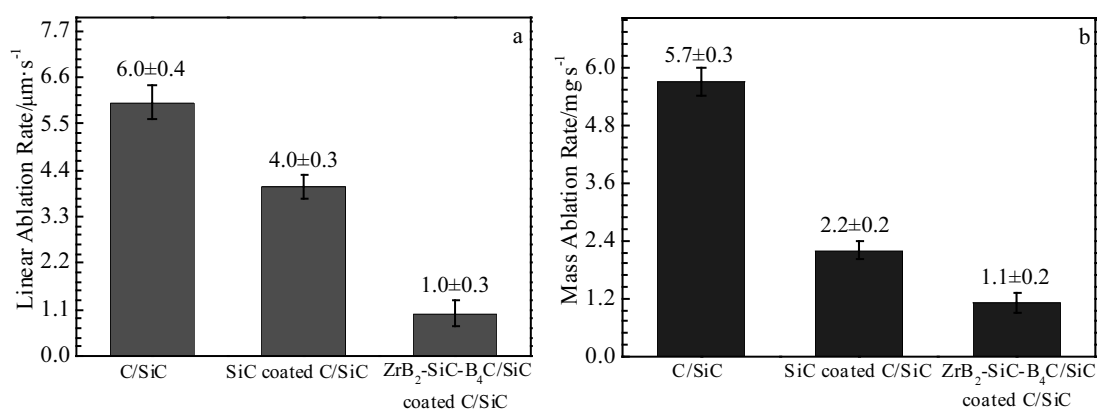
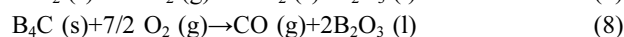
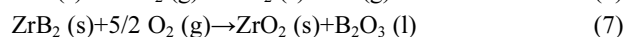
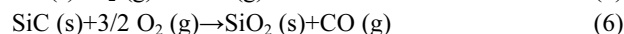


Fig.7 Linear (a) and mass (b) ablation rates of the specimens after ablation for 20 s under the heat flux of 4.2 MW/m^2

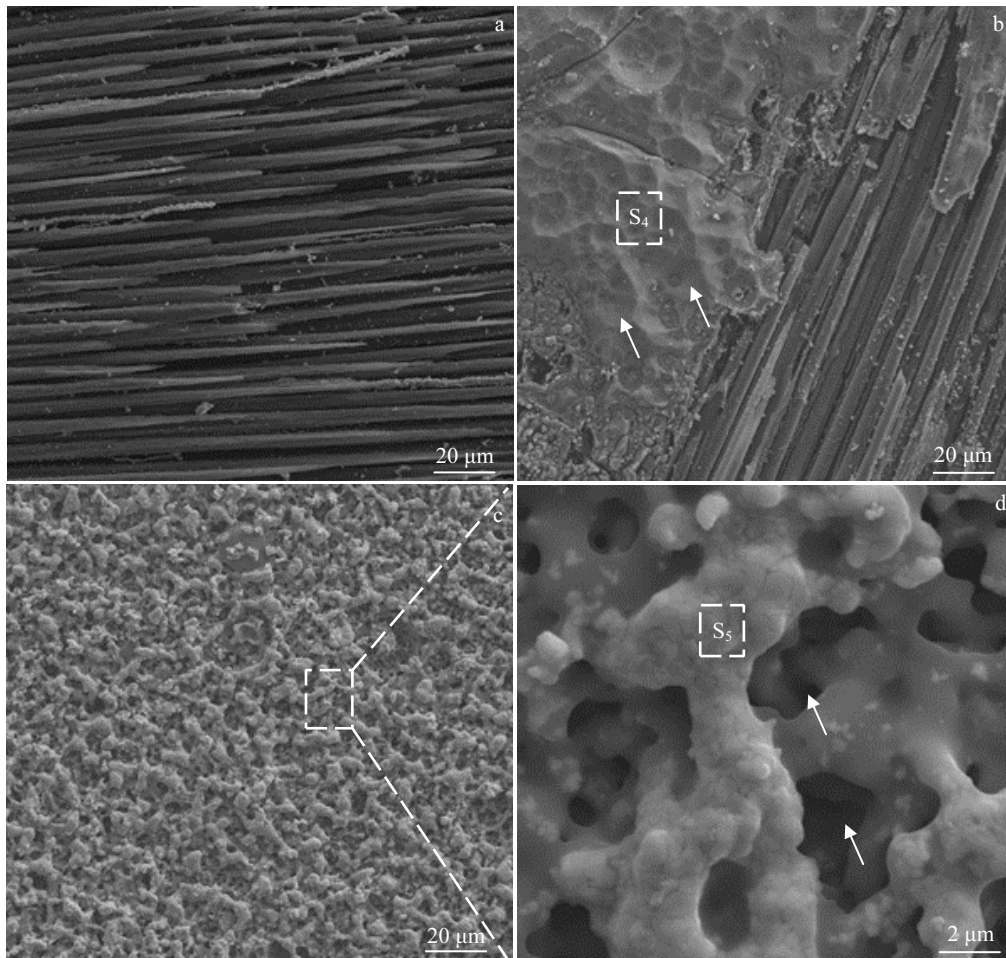


Fig.8 SEM images of the specimens after ablation: (a) C/SiC, (b) SiC coated C/SiC, and (c, d) SiC/ZrB₂-SiC-B₄C coated C/SiC



The oxidation of C/SiC composite can produce CO, CO₂ and SiO₂ (Eq.(4~6)). The oxidation reactions of carbon fibers result in mass loss, while the formation of SiO₂ causes mass gain. From Fig.4, it is found that the mass loss increases quickly at the initial oxidation period at 1500 °C for 7 h, which is mainly attributed to the oxidation of the carbon fibers. Subsequently, the mass increases slowly with the prolongation of oxidation (from 10 h to 30 h), suggesting that the carbon fibers are totally consumed and the oxidation is controlled by the formation of SiO₂ glass. As for the SiC coated C/SiC composite, the mass loss versus time follows a parabolic law. Since the oxidation of SiC coating can produce SiO₂ and CO (Eq.(6)), a layer of glassy SiO₂ forms at the initial oxidation stage. After the oxidation for 30 h, large pores appear on the coating surface, as shown in Fig.5c. Since the cracks and pores in SiO₂ layer act as high speed channels for oxygen inward diffusion, the carbon fibers are partially oxidized, as proved in Fig.5d, resulting in the quick mass loss of the composite. The oxidation curve of SiC/ZrB₂-SiC-B₄C coating

also presents a parabolic decreasing tendency. After oxidation at 1500 °C for 30 h, the mass loss ratio of SiC/ZrB₂-SiC-B₄C coating is slightly lower than that of the SiC coated C/SiC. However, the microstructure of the oxidized SiC/ZrB₂-SiC-B₄C coating is quite different. As observed in Fig.5e, the oxidation scale on the SiC/ZrB₂-SiC-B₄C coating surface is rather compact without obvious cracking. The oxidation of SiC, ZrB₂ and B₄C can produce SiO₂, ZrO₂ and B₂O₃ (Eq.(6~8)), respectively. The liquid SiO₂ can seal the porous ZrO₂, which effectively reduces the infiltration of oxygen. The mass loss depicted in Fig.4 is mainly caused by the evaporation of B₂O₃ (Eq.(9)). The formation of protective oxides of ZrO₂-SiO₂ can effectively restrict the oxygen inward diffusion, resulting in a better oxidation resistance of the composite.

3.3 Ablation mechanisms of the specimens

During ablation, the specimen center is the most severe ablation area. Thus, the following discussion is mainly focused on this area. Oxidation is an important factor that affects the specimens during ablation. For naked C/SiC

composites, the Eq.(4) and Eq.(5) can take place, resulting in the severe oxidation of carbon fibers, as shown in Fig.8a. The oxidation of single SiC coating can produce glassy SiO₂ layer (Eq.(6) and (10)). Due to the fact that the mechanical denudation at 4.2 MW/m² is extraordinarily evident^[22], the single SiO₂ oxide scale cannot resist the strong shear force from the flame under such condition, as observed in Fig.8b. Therefore, the SiC coated C/SiC suffers from serious destruction and a big ablation crater appears on the surface of C/SiC composite. In the central area of SiC/ZrB₂-SiC-B₄C coated C/SiC, after ablation for 20 s, a surface layer of ZrO₂-SiO₂ forms on the top of the oxide scale. Compared to the single SiO₂ layer, it is evident in Fig.8 that the ZrO₂-SiO₂ scale can withstand the mechanical erosion from the flame, which is attributed to the higher viscosity of the ZrO₂-SiO₂ oxides^[22-24]. As reported in Ref.[25], the formed ZrO₂ can increase melting resistance of the oxide scale, and the SiO₂ can reduce oxygen infiltration through promoting the formation of a viscous surface during ablation. With rising the surface temperature (over 1800 °C), the evolution of gases including B₂O₃, CO and SiO₂ can cause many pores on the coating surface (denoted by white arrows in Fig.8d). Based on the above analysis, compared with the pure SiC coated C/SiC composite which has been subjected to a severe destruction, the double-layered SiC/ZrB₂-SiC-B₄C coating system can effectively reduce the mass and linear ablation rates during ablation.

4 Conclusions

1) Double-layered SiC/ZrB₂-SiC-B₄C coatings can be successfully fabricated by chemical vapor deposition (CVD) and slurry painting-sintering methods. The ZrB₂-SiC-B₄C coating fabricated by two cycles of slurry painting and sintering processes is dense and intact, which has a surface roughness R_a of ~1 μm and the porosity of ~4.2%.

2) After oxidation at 1500 °C for 30 h, the mass loss ratio of SiC/ZrB₂-SiC-B₄C coated C/SiC composite is measured as ~10%. The liquid SiO₂ can seal porous ZrO₂, forming a compact oxide scale without obvious cracking, which effectively reduces the infiltration of oxygen.

3) After ablation for 20 s, the linear and mass ablation rates of SiC/ZrB₂-SiC-B₄C coating are 1.0±0.3 μm/s and 1.1±0.2 mg/s, decreased by 75.0% and 50.0% relative to those of the SiC coating, respectively. The formed ZrO₂-SiO₂ scale provides a protection against the mechanical erosion from the flame.

References

- Naslain R. *Composites Science and Technology*[J], 2004, 64(2): 155
- Zheng G B, Sano H, Uchiyama Y et al. *Journal of Materials Science*[J], 1999, 34(4): 827
- Wang Dewen, Li Cong, Meng Dongrong et al. *Rare Metal Materials and Engineering*[J], 2019, 48(7): 2317 (in Chinese)
- Huang Luming, Xiang Yang, Cao Feng et al. *Composites Part B: Engineering*[J], 2016, 86: 126
- Glime W H, Cawley J D. *Carbon*[J], 1995, 33(8): 1053
- Yang Xiang, Wei Li, Song Wang et al. *Ceramics International*[J], 2012, 38(1): 9
- Du Bin, Hong Changqing, Qu Qiang et al. *Ceramics International*[J], 2017, 43(12): 9531
- Yang Donghu, Guo Jiayi, Liu Yanbo et al. *Rare Metal Materials and Engineering*[J], 2019, 48(1): 329 (in Chinese)
- Wang Qing, Cao Feng, Xiang Yang et al. *Ceramics International*[J], 2017, 43(1): 884
- Corral E L, Loehman R E. *Journal of the American Ceramic Society*[J], 2008, 91(5): 1495
- Wang Yalei, Xiong Xiang, Li Guodong et al. *Surface and Coatings Technology*[J], 2012, 206(11-12): 2825
- Zhao Liyou, Jia Dechang, Duan Xiaoming et al. *Journal of Alloys and Compounds*[J], 2011, 509(41): 9816
- Yao D J, Li H J, Wu H et al. *Journal of the European Ceramic Society*[J], 2016, 36(15): 3739
- Wen Bo, Ma Zhuang, Liu Yanbo et al. *Ceramics International*[J], 2014, 40(8): 11 825
- Pizon D, Charpentier L, Lucas R et al. *Ceramics International*[J], 2014, 40(3): 5025
- Yang Yang, Li Kezhi, Zhao Zhigang et al. *Ceramics International*[J], 2016, 42(4): 4768
- Hu Ping, Wang Guolin, Wang Zhi. *Corrosion Science*[J], 2009, 51(11): 2724
- Zhang W Z, Zeng Y, Gbologah L et al. *Transactions of Nonferrous Metals Society of China*[J], 2011, 21(7): 1538
- Zou Xu, Fu Qiangang, Liu Lei et al. *Surface and Coatings Technology*[J], 2013, 226: 17
- Wu Heng, Li Hejun, Ma Chao et al. *Journal of the European Ceramic Society*[J], 2010, 30(15): 3267
- Qiang Xinfa, Li Hejun, Zhang Yulei et al. *Surface and Coatings Technology*[J], 2016, 307: 91
- Jia Yujun, Li Hejun, Sun Jiajia et al. *International Journal of Applied Ceramic Technology*[J], 2017, 14(3): 331
- Wang Peng, Li Sujuan, Wei Chuncheng et al. *Journal of Alloys and Compounds*[J], 2019, 781: 26
- Zhu Yan, Cheng Laifei, Ma Baisheng et al. *Ceramics International*[J], 2018, 44(7): 8166
- Jia Yujun, Li Hejun, Fu Qiangang et al. *Surface and Coatings Technology*[J], 2017, 309: 545

SiC/ZrB₂-SiC-B₄C 涂层的抗氧化和耐烧蚀性能

张宝鹏, 于新民, 刘俊鹏, 刘 伟, 霍鹏飞

(航天特种材料及工艺技术研究所, 北京 100074)

摘 要: 采用化学气相沉积 (CVD) 和浆料刷涂-烧结法制备了双层 SiC/ZrB₂-SiC-B₄C 涂层, 对比研究了无涂层、单层 SiC 涂层和双层 SiC/ZrB₂-SiC-B₄C 涂层 C/SiC 复合材料在 1500 °C 下的氧化和在 4.2 MW/m² 热流密度下的烧蚀性能。结果表明: 制备态 ZrB₂-SiC-B₄C 涂层致密、完整, 表面平均粗糙度约为 1 μm, 孔隙率约为 4.2%。在 1500 °C 氧化 30 h 后, SiC/ZrB₂-SiC-B₄C 涂层 C/SiC 复合材料的质量损失率约为 10%, 涂层表面氧化膜致密, 无明显裂纹。高温烧蚀 20 s 后, SiC/ZrB₂-SiC-B₄C 涂层的线烧蚀率和质量烧蚀率分别为 1.0±0.3 μm/s 和 1.1±0.2 mg/s, 与单层 SiC 涂层相比分别降低了 75.0% 和 50.0%, SiC/ZrB₂-SiC-B₄C 涂层烧蚀后形成的 ZrO₂-SiO₂ 氧化膜可以减缓火焰对复合材料的机械剥蚀。

关键词: C/SiC 复合材料; 涂层; 浆料刷涂; 氧化; 烧蚀

作者简介: 张宝鹏, 男, 1991 年生, 博士, 航天特种材料及工艺技术研究所, 北京 100074, 电话: 010-68743595, E-mail: bhzbp1129@buaa.edu.cn